Hindawi
Journal of Chemistry
Volume 2019, Article ID 5951793, 9 pages
https://doi.org/10.1155/2019/5951793

Research Article

Synthesis and Application of Nanomagnetic Immobilized Phospholipase C

Yang Jiang,[1] Jing Du,[2] Honglin Tang,[1] Xin Zhang,[1] Wenbin Li,[2] Liqi Wang,[3] Lianzhou Jiang,[1] and Dianyu Yu[1]

[1]*School of Food Science, Northeast Agricultural University, Harbin 150030, China*
[2]*The Key Laboratory of Soybean Biology in Chinese Ministry of Education, Northeast Agricultural University, Harbin 150030, China*
[3]*School of Computer and Information Engineering, Harbin University of Commerce, Harbin 150028, China*

Correspondence should be addressed to Dianyu Yu; dyyu2000@126.com

Received 14 October 2018; Accepted 20 January 2019; Published 3 March 2019

Guest Editor: Hiroshi Umakoshi

The nanomagnetic carrier (Fe_3O_4@SiO_2@p(GMA)) was prepared by atom transfer radical polymerization, and then, the free phospholipase C (PLC) was immobilized on it proved by the results of FT-IR analysis. The enzyme loading was 135.64 mg/g, the enzyme activity was 8560.7 U/g, the average particle size was 99.86 ± 0.80 nm, and the specific saturation magnetization was 16.00 ± 0.20 emu/g. PLC-Fe_3O_4@SiO_2@p(GMA) showed the highest activities at the pH of 7.5, and tolerance temperature raised to 65°C in soybean lecithin emulsion. Enzymatic degumming with PLC-Fe_3O_4@SiO_2@p(GMA) under the conditions of the enzyme dosage of 110 mg/kg, reaction temperature of 65°C, pH of 7.5, and reaction time of 2.5 h resulted in residual phosphorus of 64.7 mg/kg, 1,2-diacylglycerol (1,2-DAG) contents of 1.07%, and oil yield of 98.1%. Moreover, PLC-Fe_3O_4@SiO_2@p(GMA) still possessed more than 80% of its initial activity after 5 cycles.

1. Introduction

Soybean crude oil generally contains 3% of phospholipids. These need to be removed in the degumming process. The purpose of degumming removes colloidal impurities in crude oil improving the quality of it, building a good foundation for the subsequent processes [1, 2]. Phospholipids in soybean crude oil are divided into hydratable phospholipids (HPs) and nonhydratable phospholipids (NHPs). There are some differences in properties and removal process between them. HP is relatively easy to remove, while NHP is difficult to remove by water degumming [3]. In order to reduce the phosphorus content in crude oil, many factories add a large amount of phosphoric acid and alkali to remove the phospholipids, producing a lot of waste liquid, polluting the environment, and increasing the cost of oil degumming. However, enzymatic degumming effectively removes NHP from crude oil [4].

Phospholipases A_1 (PLA_1) cleaves the sn-1 ester bond of phospholipids that hydrolyzes NHP, but lysophospholipids undergo transacylation decreasing its enzymatic hydrolysis efficiency during the hydrolysis of PLA_1. Phospholipases A_2 (PLA_2) targets the sn-2 ester of phospholipids, but its enzyme activity is lower than PLA_1 and the free fatty acids produced by PLA_2 increase the acid value of soybean oil [5]. Phospholipase C (PLC) hydrolyzes the sn-3 phosphate ester bond on the glycerol side, yielding a 1,2-DAG that retains in the oil to improve oil yield and the free head group [6], so it has a good application prospect in enzymatic degumming.

The free enzyme is sensitive to temperature and pH and easily denatured under the conditions of strong acid or alkali in the process of degumming, thereby reducing the enzymatic efficiency of free enzyme. It is difficult to separate from the reaction system, and the purification procedure of it after separation is complex and expensive, which limits the application of free enzymes in oil degumming. These drawbacks can generally be overcome by immobilization. The immobilization of free enzyme improves its tolerance, stability, and easy separation from the product, and realizes the recovery and reuse of the enzyme [7]. Enzyme immobilization

methods mainly include entrapping, adsorption, covalent bonding, and cross-linking methods. The carrier materials of immobilized enzyme include natural polymer materials, synthetic polymer materials, inorganic materials, and composite materials.

As a part of immobilized enzyme, the structure and properties of carrier materials have great influence on the properties of immobilized enzyme. Therefore, many scholars have been working on the carrier material since the rise of immobilizing technology. Yu et al. found that PLA_1 was immobilized on different high molecular materials such as calcium alginate, calcium alginate-chitosan, and calcium alginate-gelatin and its catalytic performance was improved, but the viscosity of the reaction system increased due to the formation of oil residue. It brings difficulties to the separation of immobilized PLA_1 [8]. Magnetic polymer microspheres are a new type of functional biopolymer material. They are made up of magnetic materials and polymer materials, which can ensure the catalytic performance of free enzyme and the rapid separation of enzyme from the reaction system, having been widely studied. Magnetic materials generally include Fe_3O_4, $CoFe_2O_4$, Pt, Ni, and Co. Among them, Fe_3O_4 is widely studied. It combines with other modifiers to complete its surface modification so that new physical and chemical properties are more suitable for magnetic immobilization of enzymes. After magnetic immobilization of PLA_1 by Yu et al., the separation of magnetic immobilized enzyme from the reaction system was better than that of PLA_1 immobilized on polymer material [9]. Therefore, compared with polymer materials, magnetic polymer microspheres had more advantages in immobilizing enzyme.

The operational stability of the enzyme was generally improved after magnetic immobilization. Lipase and α-amylase were immobilized on magnetic carriers by Xie et al.; the thermal stability, pH stability, and storage stability of enzymes were significantly enhanced [10, 11]. Magnetic immobilized enzyme can be oriented to replace the traditional mechanical stirring under external magnetic field, avoiding the loss of enzyme on the magnetic carrier caused by mechanical stirring to improve the catalytic efficiency of immobilizing enzyme. At the same time, it can be quickly separated from the reaction system and is easy to operate. Cao et al. combined chitosan with magnetic material to immobilize papain. The results showed that the immobilized enzyme had high catalytic efficiency and was easy to separate [12]. Therefore, enzyme immobilized on a magnetic carrier can be applied to a magnetic fluidized bed, and it is easier to realize industrial continuous degumming [13].

At present, the study of PLC in oil mainly focuses on the application of free PLC in oil degumming. No article has studied the magnetic immobilization of PLC. This is the first report on magnetic immobilized PLC. In this work, a layer of SiO_x was coated on Fe_3O_4, and then, (3-aminopropyl)triethoxysilane (APTES) was used to modify the surface and attached to glycidyl methacrylate (GMA) polymer to prepare Fe_3O_4@SiO_2@p(GMA) magnetic carrier. The free PLC was immobilized on the carrier, and its characteristic absorption peak, morphological structure, particle size, and specific saturation magnetization were characterized. The enzymatic characteristics of magnetic immobilized PLC were studied, and the effect of soybean oil degumming was also investigated. It provides a theoretical basis for the application of magnetic immobilized PLC in a magnetic fluidized bed.

2. Materials and Methods

2.1. Materials. PLC, with a phospholipase activity of 17000.2 U/g, was purchased from DSM (Shanghai, China). Soybean crude oil was provided by Jiusan Group (Harbin, China) with an original phosphorus content of 802.6 mg/kg. *p*-Nitrophenylphosphorylcholine (*p*-NPPC), phosphatidylcholine (PC), and 1,2-DAG with purities greater than 98% were purchased from Sigma Chemical Ltd. (St. Louis, MO, USA). All other analytical-grade regents were from Sinopharm Chemical Reagent Co., Ltd. (Shanghai, China).

2.2. Synthesis of Fe_3O_4@SiO_2@p(GMA). Fe_3O_4 nanoparticles were prepared by chemical coprecipitation [14], the silica-coating procedure was performed by the Deng et al. [15], and APTES-modified Fe_3O_4/SiO_x nanoparticles were made by Lei et al.'s method [16]. Preparation of Fe_3O_4@SiO_2@p(GMA) with reference to Lei et al. [16] and detailed steps are as follows: 2 g of Fe_3O_4/SiO_x-g-APTES were dispersed into 30 mL of toluene containing 4 mL of triethylamine under stirring in an ice bath. A solution of 4 mL chloroacetyl chloride and 8 mL toluene was added into the dispersoid after cooling the mixture to 0°C. The mixture was stirred for 10 h at room temperature. The nanoparticles were separated with a magnet, washed with toluene and ethanol, and then dried under vacuum. 0.5 g of the above-prepared particles was dispersed in 20 mL of dimethylformamide (DMF)/water (1 : 1, mL : mL). Nitrogen was pumped into the mixture to remove oxygen for 30 min, and then [GMA]/[CuCl]/[$CuCl_2$]/[2,2′-bipyridyl](100 : 1 : 0.2 : 2) was added. The mixture was stirred with 20 r/min at room temperature for 12 h and extracted thoroughly with acetone for 48 h after the reaction; then, the samples were vacuum-dried at room temperature for 24 h.

2.3. Immobilization of PLC. The epoxy group of Fe_3O_4@SiO_2@p(GMA) forms a covalent bond with the amino group on the PLC, completing the immobilization of the PLC [16]. 1.0 g Fe_3O_4@SiO_2@p(GMA) was immersed in phosphate buffer (0.1 mol/L, pH = 7) at room temperature for 24 h. After magnetic separation, the magnetic carriers were transferred into PLC solution (0.02 g/mL, pH = 7) and stirred at 55°C for 5 h. The magnetic immobilized PLC was separated and washed with phosphate buffer (0.1 mol/L, pH = 7) three times to prepare PLC-Fe_3O_4@SiO_2@p(GMA). PLC-Fe_3O_4@SiO_2@p(GMA) was preserved at 4°C. The enzyme loading of PLC-Fe_3O_4@SiO_2@p(GMA) was detected as described by Soozanipour et al. [17].

2.4. Characterization. Fe_3O_4@SiO_2@p(GMA) and PLC-Fe_3O_4@SiO_2@p(GMA) were characterized by Fourier-

transform infrared spectrophotometer (FT-IR), X-ray diffraction (XRD), scanning electron microscope (SEM), laser particle size analyzer, and vibrating sample magnetometer (VSM).

2.5. Determination of PLC Activity. Refer to the method of Jiang et al. [18]. 1 U/mL of PLC was defined as the amount of enzyme solution needed to produce 1 nmol nitrophenol per minute by the hydrolysis of *p*-NPPC at the temperature of 36°C and the pH of 7.2. One hundred microliters of the PLC enzyme solution were added to 2 mL of *p*-NPPC solution, which contained 10 mmol/L *p*-NPPC, 250 mmol/L tris-HCl (pH 7.2), 60% sorbitol, and 1 mmol/L·$ZnCl_2$, in a test tube. The tube was incubated at 37°C for 30 min. Substrate hydrolysis was quantified by measuring absorbance at 410 nm. The activity of PLC was calculated as follows:

$$\text{activity (U/mL)} = 1.3636 \times 10^3 \times \frac{A}{t}, \quad (1)$$

where A is the absorption value at 410 nm and t is the time (in minutes) used in the substrate hydrolysis reaction. The conversion factor 1.3636×10^3 was calculated based on the standard curve of nitrophenol.

2.6. Enzymatic Characteristics of Magnetic Immobilized PLC: Effect of pH and Temperature on the Relative Activity of Magnetic Immobilized PLC. Several 4 g/100 g soybean lecithin emulsions were prepared in 0.1 mol/L phosphate buffer with different pH values. The temperature was 55°C, and the amount of free PLC or PLC-Fe_3O_4@SiO_2@p(GMA) was 2.7 mg/kg or 110 mg/kg, respectively. The effect of pH, which in the range of 5.0–8.5, on the relative activity of free PLC and PLC-Fe_3O_4@SiO_2@p(GMA) was studied. The effect of temperature on the relative activity of free PLC and PLC-Fe_3O_4@SiO_2@p(GMA) was determined using a 4 g/100 g lecithin emulsion that was soluble in 0.1 mol/L phosphate buffer with the previously determined optimum pH at temperatures ranging from 40°C to 75°C. The highest activity measured over the range of pH and temperatures was designated as 100%, and the activities at other pH and temperatures were calculated as proportions of the highest activity.

2.7. Enzymatic Degumming Process. Crude soybean oil (100.0 g) was heated to 70°C in a water bath, and 0.13 mL of 45% citric acid solution was added under high shear rate (500 rpm) for 20 min. The temperature was decreased to optimum temperature, and a 4% (w/w) NaOH solution was added to adjust the mixture pH. 3 mL deionized water and 110 mg/kg PLC-Fe_3O_4@SiO_2@p(GMA) were added to crude soybean oil. The mixture was incubated with continuous stirring at 150 rpm for 2.5 h. After the reaction, the oil mixture was quickly centrifuged at 10,000 rpm for 10 min. The residual phosphorus content in the oil phase was determined according to Yu et al. [9]. The content changes of 1,2-DAG during reaction process were researched, and the method of determination was referenced [19]. The oil yield after degumming was calculated, and the formula is as follows:

$$\text{oil yield (\%)} = \frac{M_1}{M_2} \times 100\%, \quad (2)$$

where M_1 is the quality of oil after degumming, g; M_2 is the quality of crude soybean oil, g.

Reusability of PLC-Fe_3O_4@SiO_2@p(GMA) in the process of soybean crude oil degumming was also studied. PLC-Fe_3O_4@SiO_2@p(GMA) was washed with 0.1 mol/L phosphate buffer to its optimum pH to determine the relative enzyme activity after degumming. The ratio of the residual enzyme activity to the initial enzyme activity was the relative enzyme activity.

2.8. Statistical Analysis. All experiments were carried out in triplicate to allow for the calculation of means. Statistical analysis was performed with Origin 8.5 software (OriginLab Ltd., USA).

3. Results and Discussion

3.1. Immobilization of PLC. Fe_3O_4@SiO_2@p(GMA) carrier was prepared by atom transfer radical polymerization. The reaction conditions were reaction temperature 55°C, pH 7.0, and reaction time 5 h. The effect of free PLC dosage enzyme loading and enzyme activity was investigated. The results are shown in Figure 1. When the enzyme dosage was less than 15 mL, enzyme loading and enzyme activity increased with the increase of enzyme dosage. When the enzyme dosage was more than 15 mL, enzyme loading increased slowly and the enzyme activity decreased. If the enzyme loading was high enough, it was likely that some molecules may be packed together and near enough to interact with each other reducing enzyme activity [20]. So, the optimum enzyme dosage was 15 mL, the enzyme loading of Fe_3O_4@SiO_2@p(GMA) was 135.64 mg/g, and the enzyme activity of PLC-Fe_3O_4@SiO_2@p(GMA) was 8560.7 U/g.

3.2. Characterization by FT-IR Analysis and XRD Analysis. The FT-IR analysis results of Fe_3O_4@SiO_2@p(GMA) and PLC-Fe_3O_4@SiO_2@p(GMA) are presented in Figure 2(a). The FT-IR spectroscopy of Fe_3O_4@SiO_2@p(GMA) and PLC-Fe_3O_4@SiO_2@p(GMA) had characteristic absorption peaks at 579 cm^{-1}, 1091 cm^{-1}, 1637 cm^{-1}, and 3450 cm^{-1}, respectively. The absorption peaks at 579 cm^{-1} belonged to the stretching vibration mode of FeO bonds in Fe_3O_4. The absorption peak presented at 1091 cm^{-1} was the stretching vibration of Si-O-Si bonds. The absorption peaks presented at 1637 cm^{-1} should be the stretching vibrations of -C=O bonds. The absorption peaks presented at 3450 cm^{-1} were supposed to be the stretching vibration of -OH bonds. The absorption peaks of the PLC-Fe_3O_4@SiO_2@p(GMA) presented at near 1600 cm^{-1} belonged to the amide band in protein [21]. It showed that the PLC was immobilized.

Fe_3O_4@SiO_2@p(GMA) and PLC-Fe_3O_4@SiO_2@p(GMA) were analyzed by XRD as shown in Figure 2(b). It is apparent that the diffraction pattern of Fe_3O_4@SiO_2@p(GMA) is close to PLC-Fe_3O_4@SiO_2@p(GMA). This revealed that free PLC immobilized on Fe_3O_4@SiO_2@p(GMA) did not lead to

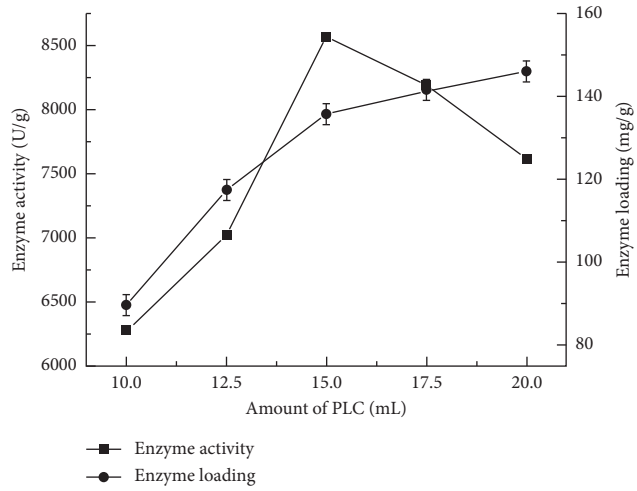

Figure 1: Effect of free PLC dosage on enzyme loading and enzyme activity. The reaction conditions were as follows: reaction temperature 55°C, pH 7.0, and reaction time 5 h. The optimum enzyme dosage was 15 mL, the enzyme loading of Fe_3O_4@SiO_2@p(GMA) was 135.64 mg/g, and the enzyme activity of PLC-Fe_3O_4@SiO_2@p(GMA) was 8560.7 U/g.

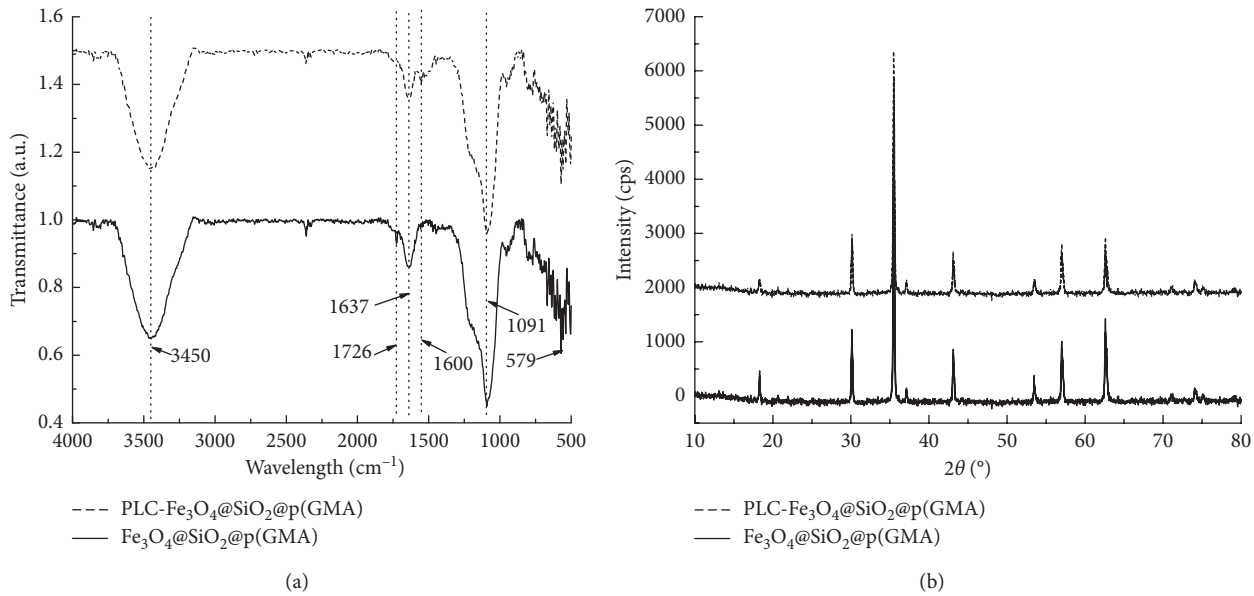

Figure 2: FT-IR spectrum analysis and XRD spectrum analysis. The FT-IR spectroscopy of Fe_3O_4@SiO_2@p(GMA) and PLC-Fe_3O_4@SiO_2@p(GMA) had characteristic absorption peaks at 579 cm^{-1}, 1091 cm^{-1}, 1637 cm^{-1}, and 3450 cm^{-1}, respectively. The absorption peaks presented at near 1600 cm^{-1} belonged to ester groups of phospholipase in the FT-IR spectroscopy of PLC-Fe_3O_4@SiO_2@p(GMA). The diffraction pattern of Fe_3O_4@SiO_2@p(GMA) was close to PLC-Fe_3O_4@SiO_2@p(GMA)'s that no phospholipase crystal peak was found in it, proving phospholipase well-dispersed on carrier. (a) FT-IR spectrum analysis. (b) XRD spectrum analysis.

Fe_3O_4 crystal structure change. However, the intensity of diffraction peak of Fe_3O_4@SiO_2@p(GMA), immobilized with PLC, decreased, which was consistent with the decrease of XRD peak intensity of immobilized enzyme by Pandey et al. [22]. It shows that the interaction between Fe_3O_4@SiO_2@p(GMA) and PLC will have some influence on the structure of Fe_3O_4@SiO_2@p(GMA).

3.3. Morphological Structure and Particle Size Analysis. The morphologies of Fe_3O_4@SiO_2@p(GMA) and PLC-Fe_3O_4@SiO_2@p(GMA) were observed by SEM. The results are shown in Figure 3(a). As shown in Figure 3(a), the ballability of Fe_3O_4@SiO_2@p(GMA) was good and the average size was 90 nm; however, some of them were agglomerated. The smaller the particle size of the nanocarrier is, the more conducive to the immobilization of enzyme was. PLC-Fe_3O_4@SiO_2@p(GMA) also had a good ballability, and the average particle size was about 105 nm as shown in Figure 3(b). Because PLC-Fe_3O_4@SiO_2@p(GMA)'s surface was uneven, this phenomenon increased the surface area of it that loaded more PLC to increase the specific activity and at the same time, increased the chance of contact between enzymes and reactants, reducing the mass transfer resistance caused by

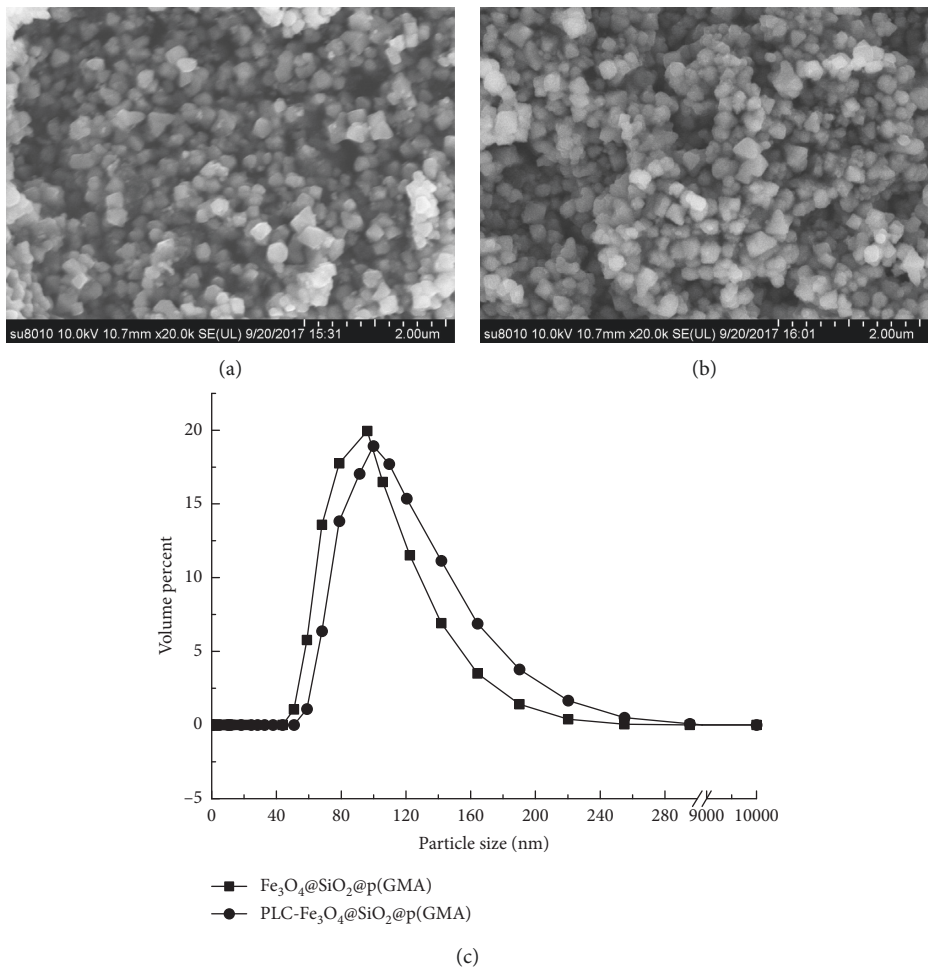

Figure 3: Scanning electron microscopy images of particles prepared and particle size analysis. In (a), the ballability of Fe_3O_4@SiO_2@p(GMA) was good and the average size was 90 nm. In (b), SEM micrographs of PLC-Fe_3O_4@SiO_2@p(GMA) also had a good ballability and the average particle size was about 105 nm. The average particle size of Fe_3O_4@SiO_2@p(GMA) was 96.70 ± 1.00 nm, and the particle size distribution range was 55 to 255 nm. For PLC-Fe_3O_4@SiO_2@p(GMA), the average particle size was 99.86 ± 0.80 nm and 90% of the particles were in the range of 58 to 295 nm. (a) Fe_3O_4@SiO_2@p(GMA). (b) PLC-Fe_3O_4@SiO_2@p(GMA). (c) Particle size analysis.

product accumulation to a certain extent [23]. Its average particle size was uniform and the diameter of it was larger than that of Fe_3O_4@SiO_2@p(GMA), indicating that the immobilization effect of PLC-Fe_3O_4@SiO_2@p(GMA) was fine.

Determination of particle size of Fe_3O_4@SiO_2@p(GMA) and PLC-Fe_3O_4@SiO_2@p(GMA) by using the laser particle size analyzer is shown in Figure 3(c).

When the laser passes through the moving particles, the light scattering will occur and the frequency of the scattering light will cause Doppler shift. The particle size can be calculated by measuring the spectrum half width of scattered light intensity. In the graph, the average particle size of the Fe_3O_4@SiO_2@p(GMA) was 96.70 ± 1.00 nm, larger than the particle size measured by the SEM, the polydispersity index (PDI) was 0.245, and the particle size distribution range was 55 to 255 nm that had a wide range. The average particle size of PLC-Fe_3O_4@SiO_2@p(GMA) had a concentrated distribution range. 90% of the particles were in the range of 58 to 295 nm. The average particle size was 99.86 ± 0.80 nm that was smaller than the particle size measured by SEM, and PDI was 0.293. The number of particles between 60~80 nm, 80~100 nm, 100~120 nm, and 120~160 nm were 20%, 35%, 32%, and 14%, respectively, which showed that the particles were concentrated in the area with larger particle size. PLC-Fe_3O_4@SiO_2@p(GMA) was a kind of nanoparticles as a result of its particle size [16].

3.4. Magnetic Analysis. Figure 4 shows that the specific saturation magnetization of Fe_3O_4@SiO_2@p(GMA) and PLC-Fe_3O_4@SiO_2@p(GMA) was analyzed by VSM. The specific saturation magnetization was found to be 19.70 ± 0.60 emu/g and 16.00 ± 0.20 emu/g for Fe_3O_4@SiO_2@p(GMA) and PLC-Fe_3O_4@SiO_2@p(GMA), respectively. The specific saturation magnetization of PLC-Fe_3O_4@SiO_2@p(GMA) decreased, and it may be that PLC reduced the specific saturation magnetization of the carrier after immobilizing. However, they could be well magnetized under external magnetic field, which was conducive to regular movement in the magnetic reactor. Remanence and

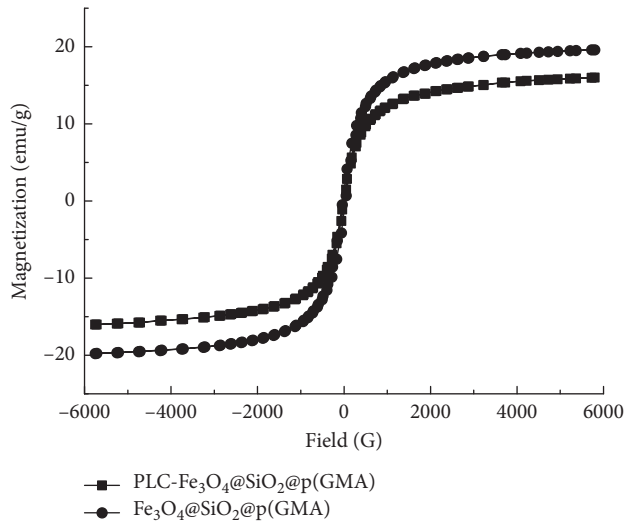

Figure 4: Magnetic hysteresis loop. The specific saturation magnetization was found to be 19.70 ± 0.60 emu/g and 16.00 ± 0.20 emu/g for Fe_3O_4@SiO_2@p(GMA) and PLC-Fe_3O_4@SiO_2@p(GMA), respectively.

coercivity of Fe_3O_4@SiO_2@p(GMA) and PLC-Fe_3O_4@SiO_2@p(GMA) were almost zero, resulting in them having no remanence and agglomeration when the external magnetic field was removed [24]. The results can realize redispersion and subsequent separation of PLC-Fe_3O_4@SiO_2@p(GMA) in a magnetically fluidized bed.

3.5. Enzymatic Characteristics of Nanomagnetic Immobilized PLC: Effect of pH and Temperature on the Relative Activity of Nanomagnetic Immobilized PLC. The effect of pH on the relative activity of nanomagnetic immobilized PLC was determined, and the results are shown in Figure 5(a). As shown in Figure 5(a), the maximum relative activity of free PLC was obtained at pH 6.5 (12124.7 U/g). PLC-Fe_3O_4@SiO_2@p(GMA) possessed maximum relative activity at pH 7.5 (7547.5 U/g) that retained more than 80% relative activity in the pH range of 6.0–8.5. So, the optimum pH was shifted, and the tolerance pH range was obviously wider than that of free PLC after immobilizing. Magnetic carriers attached to negative charges since a large number of carboxyl groups may have existed on the surface of Fe_3O_4@SiO_2@p(GMA), attracted cations, including H^+, and attached them to the surface of the carrier. As a result, the concentration of H^+ in the diffusion layer was higher than that in the surrounding solution. The pH in the external solution shifted to alkalinity in order to counteract the microenvironmental effect to make the enzyme show maximum activity. So, the optimum pH of PLC-Fe_3O_4@SiO_2@p(GMA) has a shift toward the alkaline side, which also proves that PLC has been immobilized on Fe_3O_4@SiO_2@p(GMA) [25]. This result is consistent with the migration direction of optimum pH after magnetic immobilization of PLA_2 by Qu et al. [26]. When pH was 7.5, the enzyme activity of PLC-Fe_3O_4@SiO_2@p(GMA) was the highest, probably because the pH was close to its isoelectric point, which enhanced its tolerance in the alkaline environment. It may also be that there was a sufficiently stable covalent bond between PLC and Fe_3O_4@SiO_2@p(GMA) to resist the conformation change of PLC and to reduce the dissociation rate of PLC. When pH was greater than 7.5, the reduction of enzyme activity may be due to the abscission of PLC on the carrier. Accordingly, the optimum pH of PLC-Fe_3O_4@SiO_2@p(GMA) was 7.5.

The effect of temperature on the relative activity of nanomagnetic immobilized PLC to hydrolyze soybean lecithin emulsions was determined, and the results are shown in Figure 5(b). The maximum relative activity of free PLC was at 55°C (11043.8 U/g), while that of PLC-Fe_3O_4@SiO_2@p(GMA) was at 65°C (7693.8 U/g) that had more than 80% of the initial activity in the range of 50°C–70°C. It demonstrated that immobilized PLC had a wider tolerance for temperature. Stability of immobilized enzyme depends on the immobilization strategy. Free PLC was connected with Fe_3O_4@SiO_2@p(GMA) in covalent bond and changed the secondary structure of free PLC, increasing the rigidity of PLC structure, changing the conformation of immobilized enzyme that made it more suitable for contact with substrate, reducing the denaturant at high temperature, and improving its thermal stability [27, 28]. Defaei et al. immobilized α-amylase onto naringin functionalized MNPs that exhibited a good thermostability [29]. *Candida antarctica* lipase B was immobilized on Fe_3O_4@SiO_2@p(GMA); its optimum temperature was increased by 5°C and had higher activities at a wider range of temperatures [30]. The results suggest that the optimum temperature of PLC is increased by 10°C through immobilizing.

3.6. Enzymatic Degumming Process. The content changes of residual phosphorus and 1,2-DAG in reaction are shown in Figure 6. Within 0–1.0 h, the content of residual phosphorus decreased rapidly and nevertheless, the content of 1,2-DAG increased rapidly. There was a slow reduction in residual phosphorus content, but 1,2-DAG content continued to increase at the same time when reaction time was from 1.0 h to 2.0 h. PLC-Fe_3O_4@SiO_2@p(GMA) reacted in crude soybean oil for 2.0 h, and the residual phosphorus and 1,2-DAG were 64.7 mg/kg and 1.07%, respectively. The oil yield after degumming was 98.1%, which was about 1.0% higher than that of water degumming oil [18]. When the reaction time continued to prolong, the change of residual phosphorus and 1,2-DAG was not significant. The main reason was that PLC-Fe_3O_4@SiO_2@p(GMA) hydrolyzed PC and phosphatidyl ethanolamines (PE) to produce 1,2-DAG in crude soybean oil at the beginning of reaction [31], and there was no remarkable change in residual phosphorus and 1,2-DAG on account of the substrate decreased gradually. As clearly seen here, PLC-Fe_3O_4@SiO_2@p(GMA) can be applied to crude soybean oil degumming.

3.7. Reusability of Nanomagnetic Immobilized PLC in Degumming. Reusability of nanomagnetic immobilized PLC in degumming is shown in Figure 7. PLC-Fe_3O_4@SiO_2@p(GMA) had 82.5% relative activity after 5 recycles.

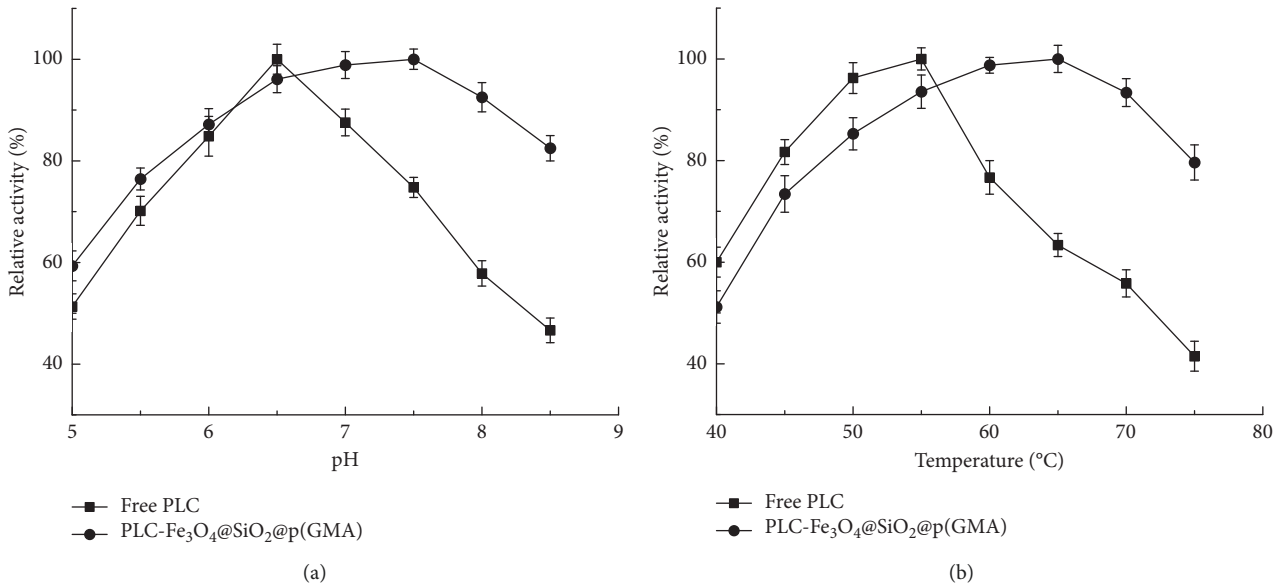

Figure 5: Effect of pH and temperature on the relative activity of free PLC and PLC-Fe_3O_4@SiO_2@p(GMA). Effect of pH on the relative activity of free PLC and PLC-Fe_3O_4@SiO_2@p(GMA) using soybean lecithin emulsions as a substrate at 55°C for 2 h. The optimum pH of PLC was 7.5 after immobilizing. Effect of temperature on the relative activity of free PLC and PLC-Fe_3O_4@SiO_2@p(GMA), hydrolyzing soybean lecithin emulsions, was determined within pH 6.5 and 7.5 for 2 h The optimum temperatures of PLC were increased by 10°C through immobilizing. The data were reproduced three times, and error bars indicate standard deviations. (a) Effect of pH on the relative activity of free PLC and PLC-Fe_3O_4@SiO_2@p(GMA). (b) Effect of temperature on the relative activity of free PLC and PLC-Fe_3O_4@SiO_2@p(GMA).

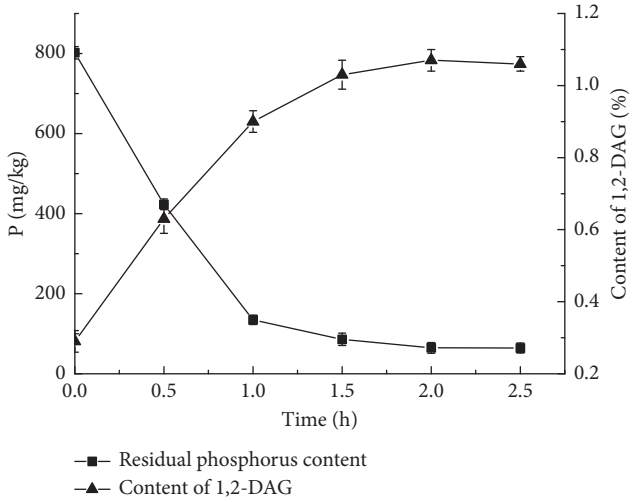

Figure 6: Content of residual phosphorus and 1,2-DAG changes with time. The degumming conditions were at 65°C and pH of 7.5 for 2.5 h in crude soybean oil. After reacting for 2.0 h in crude soybean oil, the residual phosphorus and 1,2-DAG were 64.7 mg/kg and 1.07%, respectively. The data were reproduced three times, and error bars indicate standard deviations.

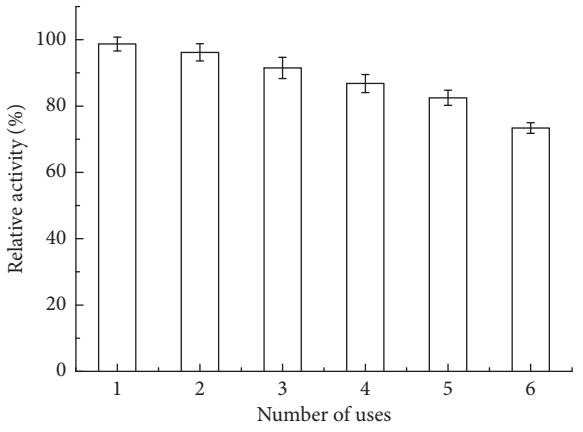

Figure 7: Reusability of PLC-Fe_3O_4@SiO_2@p(GMA), using crude soybean oil as a substrate at 65°C with a pH of 7.5 for 2.5 h. PLC-Fe_3O_4@SiO_2@p(GMA) retained 82.5% relative activity after 5 recycles. The data were reproduced three times, and error bars indicate standard deviations.

The relative activity of it was 73.4% after 6 recycles. So, PLC-Fe_3O_4@SiO_2@p(GMA) exhibited a good reusability. The research of Segato et al. showed that immobilized cellobiohydrolase D (CelD) retained more than 80% of its initial activity after 4 consecutive reuses [32]. The loss of enzyme activity was attributed to the denaturation of PLC in the hydrolysis environment, followed by the mechanical agitation and the collision of magnetic immobilized PLC during hydrolysis, which resulted in the PLC shedding off the carrier [9]. So, magnetic immobilized enzymes have good reusability.

4. Conclusion

In this experiment, the free PLC was immobilized on the Fe_3O_4@SiO_2@p(GMA) carrier. PLC-Fe_3O_4@SiO_2@p(GMA) had high enzyme loading and enzyme activity. It had a good ballability as nanoparticles and high specific saturation magnetization that quickly separated from the reaction

system. The enzymatic properties of PLC-Fe_3O_4@SiO_2@p(GMA) showed that the tolerance pH range was widened and the tolerance temperature increased by 10°C. Phospholipids were converted to 1,2-DAG in degumming, which increased the oil yield about 1.0%, and PLC-Fe_3O_4@SiO_2@p(GMA) had good reusability. So, PLC-Fe_3O_4@SiO_2@p(GMA) can be used in the degumming of oil in a magnetic fluidized bed.

Data Availability

The data used to support the findings of this study are available from the corresponding author upon request.

Conflicts of Interest

The authors declare that there are no conflicts of interest regarding the publication of this paper.

Acknowledgments

This work was supported by a grant from the National Natural Science Foundation of China (NSFC), "Study on the Mechanism of Nanomagnetic Enzyme Hydrolysis of Soy-Bean Oil by Multi-Effect Orientation and Biosynthesis of Functional Lipids" (No. 31571880). This work was also supported by a grant from "Rice Bran High-Value Steady-State Processing Technology and Intelligent Equipment Research and Demonstration" (No. 2018YFD0401101).

References

[1] G. Gofferjé, J. Motulewicz, A. Stäbler, T. Herfellner, U. Schweiggert-Weisz, and E. Flöter, "Enzymatic degumming of crude jatropha oil: evaluation of impact factors on the removal of phospholipids," *Journal of the American Oil Chemists' Society*, vol. 91, no. 12, pp. 2135–2141, 2014.

[2] C. Elena, S. Cerminati, P. Ravasi et al., "*B. cereus* phospholipase C engineering for efficient degumming of vegetable oil," *Process Biochemistry*, vol. 54, pp. 67–72, 2017.

[3] X. Jiang, M. Chang, X. Wang, Q. Jin, and X. Wang, "A comparative study of phospholipase A_1 and phospholipase C on soybean oil degumming," *Journal of the American Oil Chemists' Society*, vol. 91, no. 12, pp. 2125–2134, 2014.

[4] D. L. Lamas, D. T. Constenla, and D. Raab, "Effect of degumming process on physicochemical properties of sunflower oil," *Biocatalysis and Agricultural Biotechnology*, vol. 6, pp. 138–143, 2016.

[5] D. L. Lamas, G. H. Crapiste, and D. T. Constenla, "Changes in quality and composition of sunflower oil during enzymatic degumming process," *LWT-Food Science and Technology*, vol. 58, no. 1, pp. 71–76, 2014.

[6] M. S. Piel, G. H. J. Peters, and J. Brask, "Chemoenzymatic synthesis of fluorogenic phospholipids and evaluation in assays of phospholipases A, C and D," *Chemistry and Physics of Lipids*, vol. 202, pp. 49–54, 2017.

[7] D. Yu, Y. Ma, L. Jiang et al., "Stability of soybean oil degumming using immobilized phospholipase A_2," *Journal of Oleo Science*, vol. 63, no. 1, pp. 25–30, 2014.

[8] D. Yu, L. Jiang, Z. Li, J. Shi, J. Xue, and Y. Kakuda, "Immobilization of phospholipase A_1 and its application in soybean oil degumming," *Journal of the American Oil Chemists' Society*, vol. 89, no. 4, pp. 649–656, 2011.

[9] D. Yu, Y. Ma, S. J. Xue, L. Jiang, and J. Shi, "Characterization of immobilized phospholipase A_1 on magnetic nanoparticles for oil degumming application," *LWT-Food Science and Technology*, vol. 50, no. 2, pp. 519–525, 2013.

[10] W. Xie and J. Wang, "Enzymatic production of biodiesel from soybean oil by using immobilized lipase on Fe_3O_4/poly(styrene-methacrylic acid) magnetic microsphere as a biocatalyst," *Energy & Fuels*, vol. 28, no. 4, pp. 2624–2631, 2014.

[11] H. Guo, Y. Tang, Y. Yu, L. Xue, and J.-q. Qian, "Covalent immobilization of α-amylase on magnetic particles as catalyst for hydrolysis of high-amylose starch," *International Journal of Biological Macromolecules*, vol. 87, pp. 537–544, 2016.

[12] S.-L. Cao, X.-H. Li, W.-Y. Lou, and M.-H. Zong, "Preparation of a novel magnetic cellulose nanocrystal and its efficient use for enzyme immobilization," *Journal of Materials Chemistry B*, vol. 2, no. 34, pp. 5522–5530, 2014.

[13] K. Atacan, B. Çakıroğlu, and M. Özacar, "Improvement of the stability and activity of immobilized trypsin on modified Fe_3O_4 magnetic nanoparticles for hydrolysis of bovine serum albumin and its application in the bovine milk," *Food Chemistry*, vol. 212, pp. 460–468, 2016.

[14] H. Meng, Z. Zhang, F. Zhao, T. Qiu, and J. Yang, "Orthogonal optimization design for preparation of Fe_3O_4 nanoparticles via chemical coprecipitation," *Applied Surface Science*, vol. 280, no. 8, pp. 679–685, 2013.

[15] Y.-H. Deng, C.-C. Wang, J.-H. Hu, W.-L. Yang, and S.-K. Fu, "Investigation of formation of silica-coated magnetite nanoparticles via sol-gel approach," *Colloids and Surfaces A: Physicochemical and Engineering Aspects*, vol. 262, no. 1–3, pp. 87–93, 2005.

[16] L. Lei, X. Liu, Y. Li, Y. Cui, Y. Yang, and G. Qin, "Study on synthesis of poly(GMA)-grafted Fe_3O_4/SiO_X magnetic nanoparticles using atom transfer radical polymerization and their application for lipase immobilization," *Materials Chemistry & Physics*, vol. 125, no. 3, pp. 866–871, 2011.

[17] A. Soozanipour, A. Taheri-Kafrani, and A. Landarani Isfahani, "Covalent attachment of xylanase on functionalized magnetic nanoparticles and determination of its activity and stability," *Chemical Engineering Journal*, vol. 270, pp. 235–243, 2015.

[18] X. Jiang, M. Chang, Q. Jin, and X. Wang, "Application of phospholipase A_1 and phospholipase C in the degumming process of different kinds of crude oils," *Process Biochemistry*, vol. 50, no. 3, pp. 432–437, 2015.

[19] P. Ravasi, M. Braia, F. Eberhardt et al., "High-level production of Bacillus cereus phospholipase C in Corynebacterium glutamicum," *Journal of Biotechnology*, vol. 216, pp. 142–148, 2015.

[20] L. Fernandez-Lopez, S. G. Pedrero, N. Lopez-Carrobles, B. C. Gorines, J. J. Virgen-Ortíz, and R. Fernandez-Lafuente, "Effect of protein load on stability of immobilized enzymes," *Enzyme and Microbial Technology*, vol. 98, pp. 18–25, 2017.

[21] J. Yang, L. Zhong, B. Zou et al., "Spectroscopic investigations on the binding of persimmon tannin to phospholipase A_2 from Chinese cobra (Naja naja atra)," *Journal of Molecular Structure*, vol. 1008, pp. 42–48, 2012.

[22] G. Pandey, D. M. Munguambe, M. Tharmavaram et al., "Halloysite nanotubes-an efficient 'nano-support' for the immobilization of α-amylase," *Applied Clay Science*, vol. 136, pp. 184–191, 2017.

[23] L. Zhang and Y. Sun, "Poly(carboxybetaine methacrylate)-grafted silica nanoparticle: a novel carrier for enzyme

immobilization," *Biochemical Engineering Journal*, vol. 132, pp. 122–129, 2018.

[24] F. Guo, Q. Zhang, B. Zhang, H. Zhang, and L. Zhang, "Preparation and characterization of magnetic composite microspheres using a free radical polymerization system consisting of DPE," *Polymer*, vol. 50, no. 8, pp. 1887–1894, 2009.

[25] Q. Liu, Y. Hua, X. Kong, C. Zhang, and Y. Chen, "Covalent immobilization of hydroperoxide lyase on chitosan hybrid hydrogels and production of C6 aldehydes by immobilized enzyme," *Journal of Molecular Catalysis B: Enzymatic*, vol. 95, pp. 89–98, 2013.

[26] Y. Qu, L. Sun, X. Li et al., "Enzymatic degumming of soybean oil with magnetic immobilized phospholipase A_2," *Lebensmittel-Wissenschaft & Technologie*, vol. 73, pp. 290–295, 2016.

[27] A. Sanchez, J. Cruz, N. Rueda et al., "Inactivation of immobilized trypsin under dissimilar conditions produces trypsin molecules with different structures," *RSC Advances*, vol. 6, no. 33, pp. 27329–27334, 2016.

[28] M. Y. Arıca, "Immobilization of polyphenol oxidase on carboxymethylcellulose hydrogel beads: preparation and characterization," *Polymer International*, vol. 49, no. 7, pp. 775–781, 2000.

[29] M. Defaei, A. Taheri-Kafrani, M. Miroliaei, and P. Yaghmaei, "Improvement of stability and reusability of α-amylase immobilized on naringin functionalized magnetic nanoparticles: a robust nanobiocatalyst," *International Journal of Biological Macromolecules*, vol. 113, pp. 354–360, 2018.

[30] D. Yu, X. Zhang, D. Zou et al., "Immobilized CALB catalyzed transesterification of soybean oil and phytosterol," *Food Biophysics*, vol. 13, no. 2, pp. 208–215, 2018.

[31] C. Elena, P. Ravasi, S. Cerminati, S. Peiru, M. E. Castelli, and H. G. Menzella, "Pichia pastoris, engineering for the production of a modified phospholipase C," *Process Biochemistry*, vol. 51, no. 12, pp. 1934–1944, 2016.

[32] F. Segato, M. Wilkins, R. Prade et al., "Cellulase immobilization on superparamagnetic nanoparticles for reuse in cellulosic biomass conversion," *AIMS Bioengineering*, vol. 3, no. 3, pp. 264–276, 2016.